



Positron Production from Betatron X-rays Emitted in a Plasma Wiggler

Devon K Johnson

Electrical Engineering Department, UCLA

Advanced Accelerator Concepts 2006

7/12/2006

** Part of the E-167 collaboration at SLAC*



Experimental Collaborators



- This work was performed parasitically to the Plasma Wakefield Accelerator Experiment (PWFA) at the Stanford Linear Accelerator Center (SLAC)

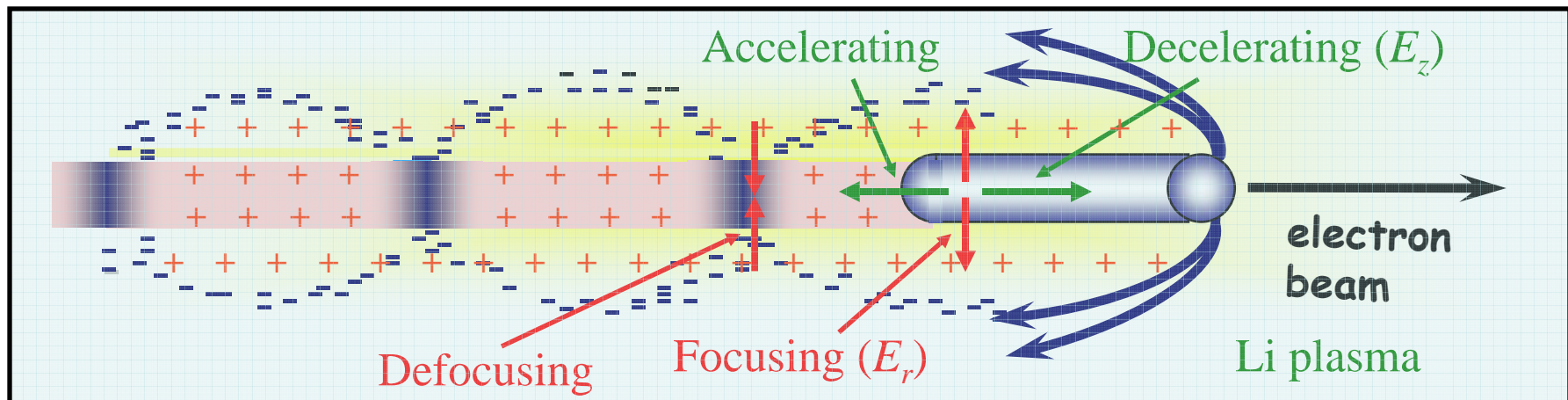


Figure 1: PWFA Experimental Schematic

- The complete list of E-167 experimental collaborators
D.K. Johnson¹, D. Auerbach¹, I. Blumenfeld², C.D. Barnes², C.E. Clayton¹, F.J. Decker², S. Deng³, P. Emma², M.J.Hogan², C. Huang¹, R. Ischebeck², R. Iverson², C. Joshi¹, T.C. Katsouleas³, N. Kirby², P. Krejcik², W. Lu¹, K.A. Marsh¹, W.B. Mori¹, P. Muggli³, E. Oz³, R.H. Siemann², C.L. O'Connell², D. Walz², M. Zhou¹

⁽¹⁾ University of California, Los Angeles, CA 90095, USA

⁽²⁾ Stanford Linear Accelerator Center, Stanford, CA 94309, USA

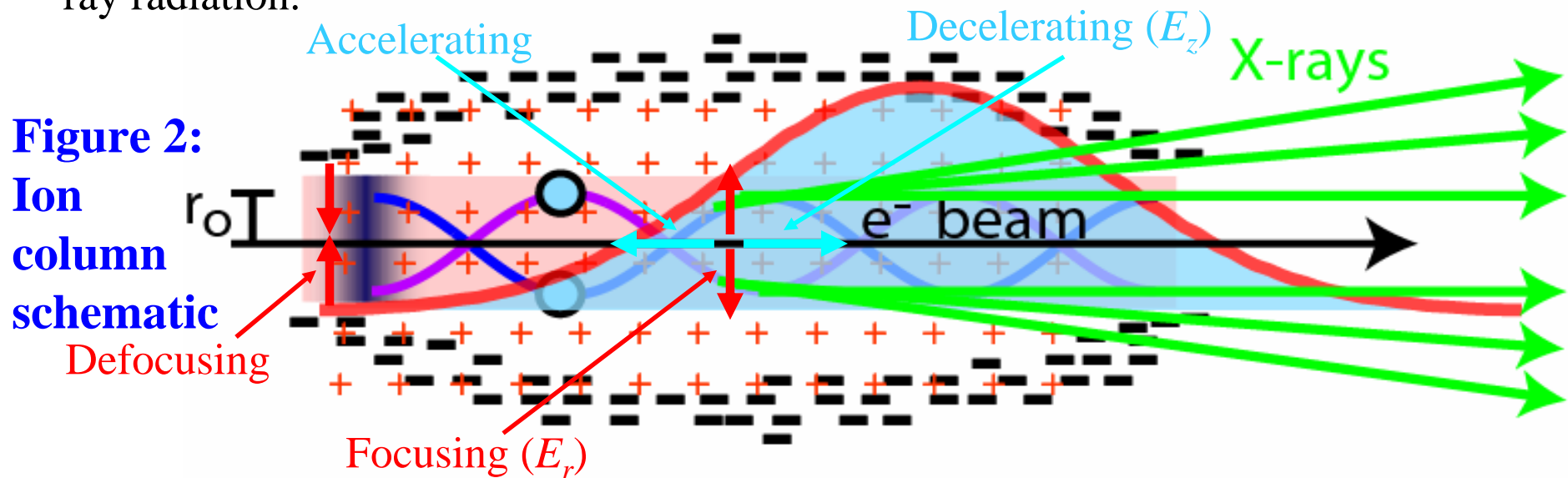
⁽³⁾ University of Southern California, Los Angeles, CA 90089, USA



Plasma Wiggler for MeV X-ray Production



- If $n_b > n_{pe}$, all plasma e^- are blown-out creating an ion column.
- Plasma ion column acts as a “Plasma Wiggler”, causing betatron motion and X-ray radiation.



Typical Parameters:

$n_{pe} = 3 \times 10^{17} \text{ cm}^{-3}$,

$\gamma = 56000$, $r_0 = 10 \text{ } \mu\text{m}$:

Giving:

$E_r = 27 \text{ GV/m}$, $\lambda_\beta = 2 \text{ cm}$

$B/r = 9 \text{ MT/m}$

Wiggler strength: $K = \frac{\gamma \omega_\beta}{c} r_0 = f(\sqrt{n_p}, r_0, \sqrt{\gamma}) = 173$

Critical frequency on-axis ($K \gg 1$): $\omega_c = \frac{3 \omega_\beta^2 \gamma^3}{2c} r_0 = f(n_p, r_0, \gamma^2) = 49.6 \text{ MeV}$

Larmor Formula Energy Loss: $\frac{dE}{dz} = \frac{1}{3} r_e m_e c^2 \gamma^2 k_\beta^2 K^2 = f(n_p^2, r_0^2, \gamma^2) = 4.3 \text{ GeV/m}$

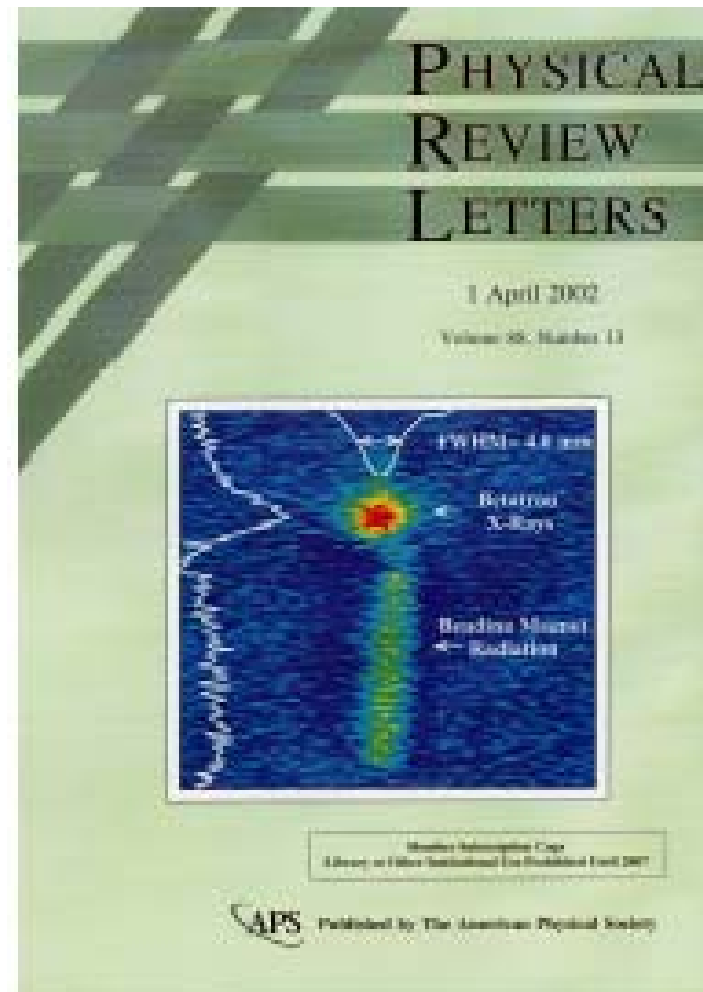


Previous Plasma X-Ray Observation



- During previous experiments performed by UCLA student Shoquin Wang at SLAC, betatron oscillations and plasma X-rays were observed
 - 1) $n_{pe} = 10^{14} \text{ cm}^{-3}$
 - 2) X-rays measured were in the **5-30 KeV** range
- Phosphor Image of X-rays
 - 1) Betatron X-rays (red spot)
 - 2) Bending radiation from e^- extraction (green and yellow stripe)

S. Wang et al. Phys. Rev. Lett. Vol 88. Num 13, pg. 135004, (2002)





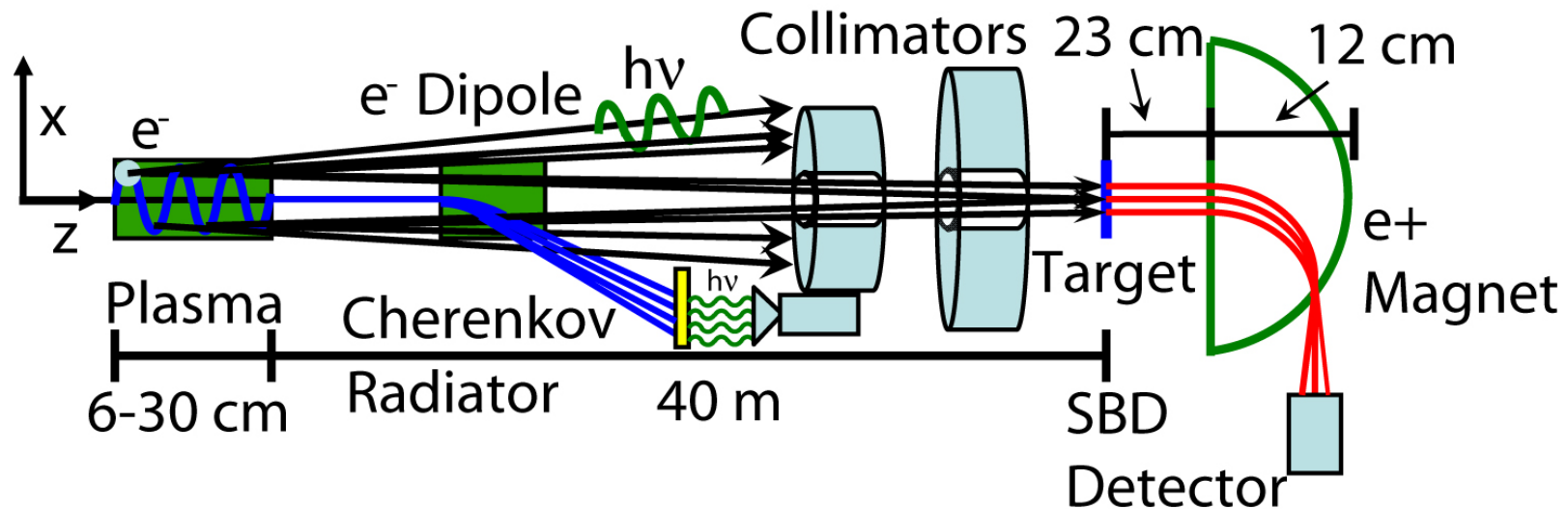
Positron Experimental Setup



UCLA



Figure 4: Positron Experimental Schematic

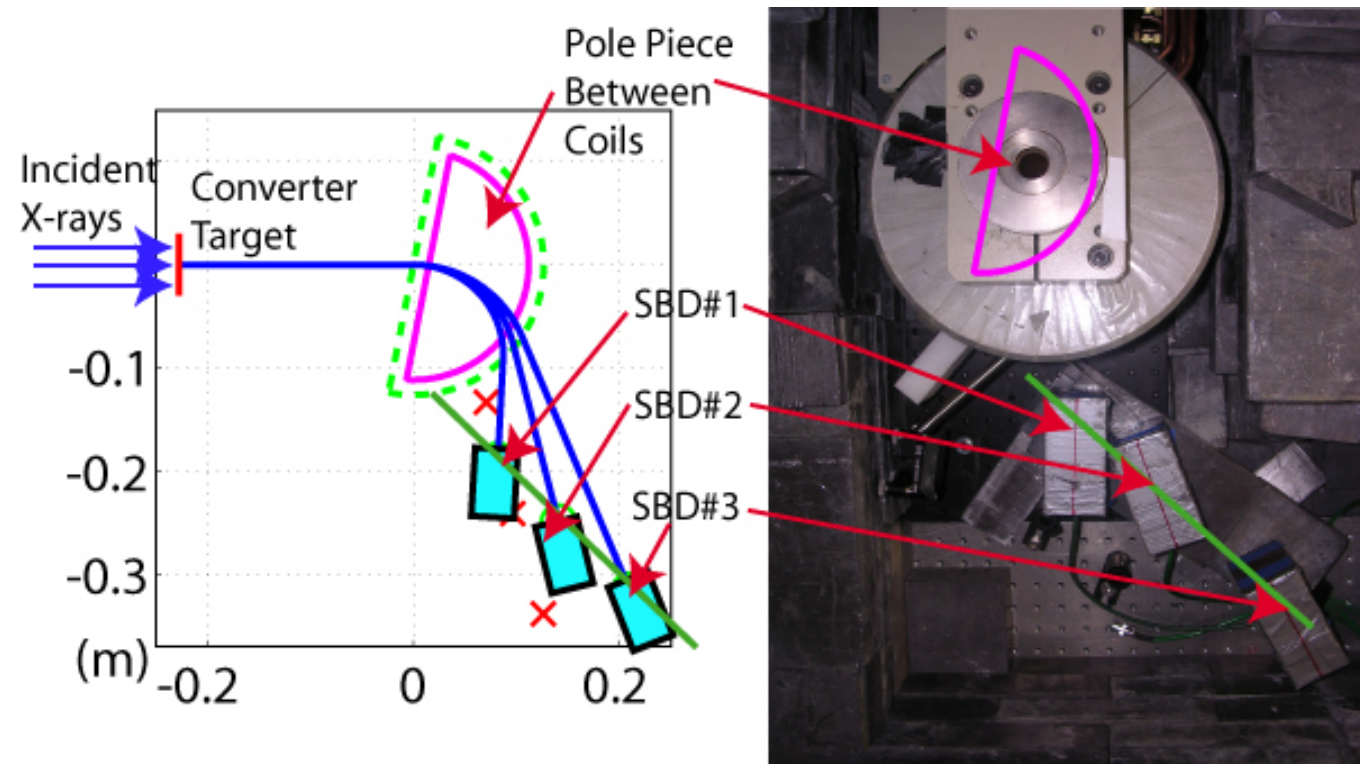


- Radiated X-rays travel 40 m to e^+ experiment.
- With $n_{pe}=3 \times 10^{17} \text{ cm}^{-3}$, $\theta = K/\gamma = 9 \text{ mrad}$.
- Collimate X-ray beam to $\theta = 0.2 \text{ mrad}$ ($r = 4 \text{ mm}$)
- Most high energy photons within $\theta = 1/\gamma = 0.02 \text{ mrad}$
- Only about 5% of the radiated X-ray energy hits the target.
- Target is 1.7mm thick ($0.5X_0$) Tungsten (W).



Figure 5: Positron Detector Setup

- A semicircular pole piece.
- 11 degree pole face rotation.
- Data collection with 1mm thick Silicon Surface Barrier Detectors (SBDs).
- SBDs in the vertical focal plane (green line).





Positron/Electron Data

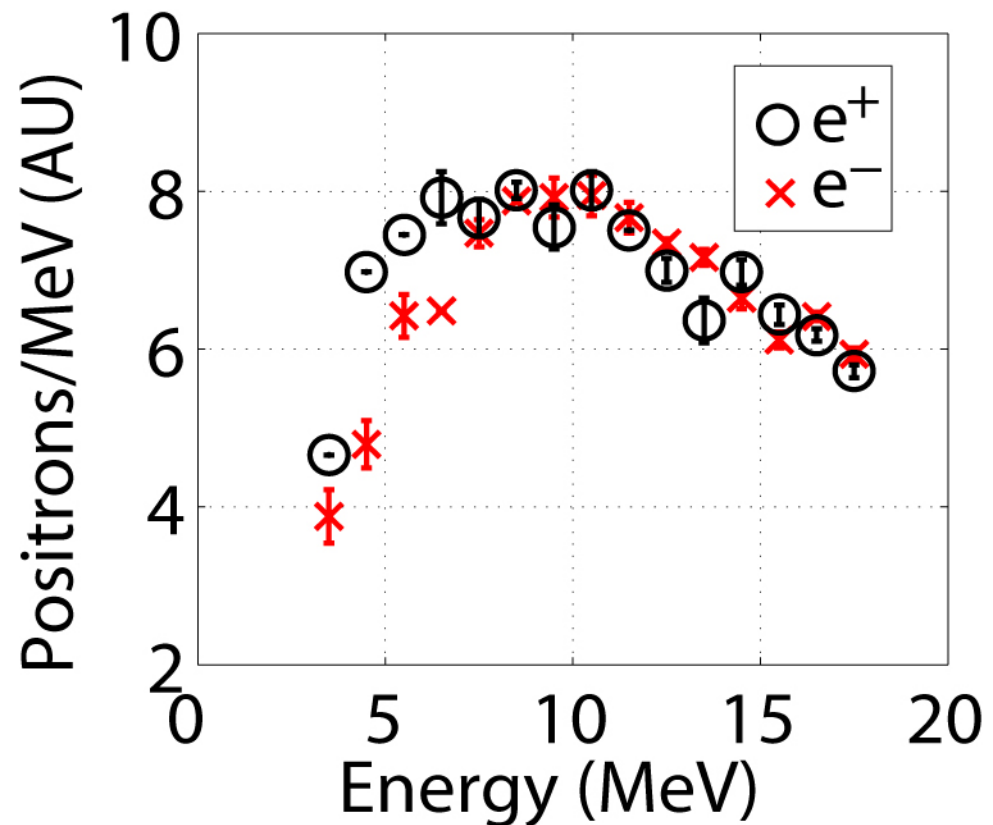


UCLA



Figure 6: Typical Measured Electron and Positron Spectra

- Most data was taken with just positrons
- The polarity of the magnet was changed to measure electrons
- This provides proof that the target was creating the pairs
- The variations between the two spectra are due to shot-to-shot linac variations.





Calculation of the X-ray Spectrum

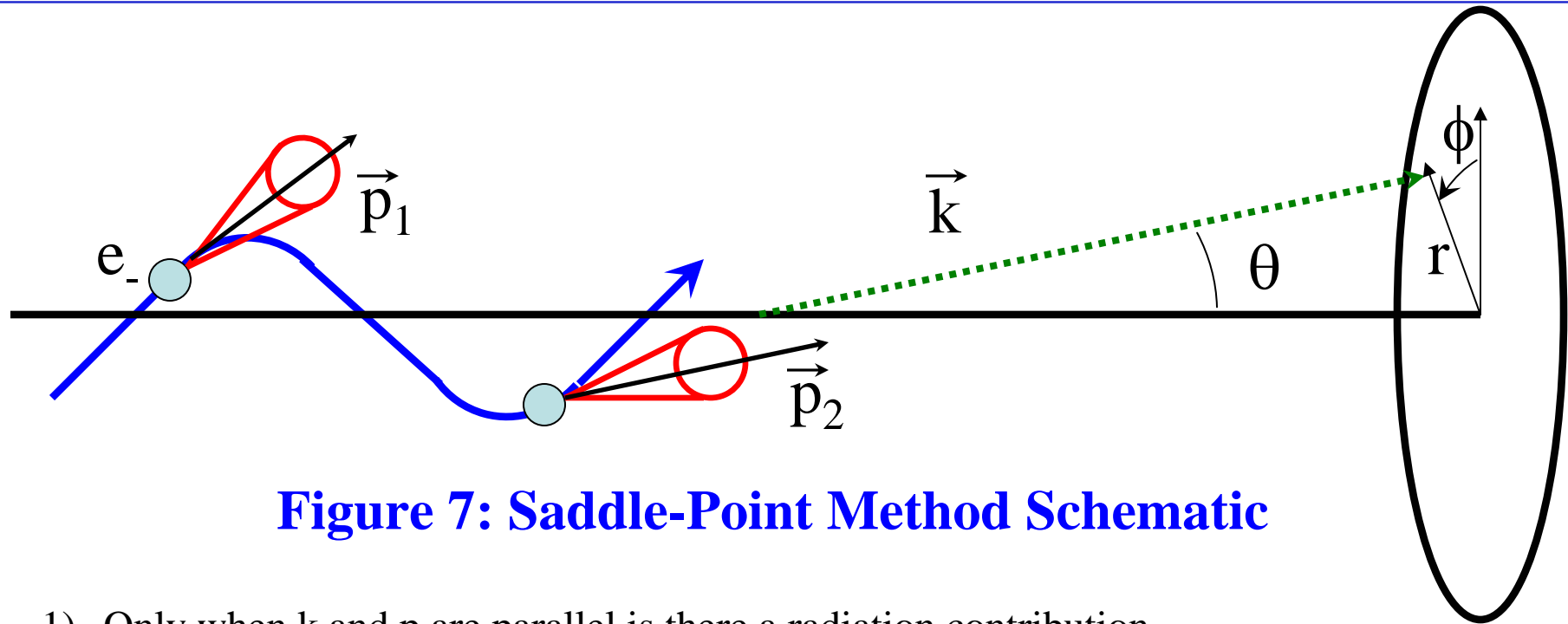


Figure 7: Saddle-Point Method Schematic

- 1) Only when k and p are parallel is there a radiation contribution.
- 2) This “saddle-point” has a characteristic radius of curvature.
- 3) This gives a characteristic “synchrotron-like” radiation spectrum
- 4) Approximates the radiation field to that of a particle moving in a circular path.

Assumption: The electron deflection angle (p_x/p_z) should be much larger than the angular spread of the radiation ($1/\gamma$) – (Kostyukov et al, Phys Plasmas, 10, 2003)

$$\gamma \gg K = \gamma k_\beta r \gg 1$$



Photon and Energy Spectrum



- The energy spectrum and the integrated energy spectrum for *one* e^- ($r_\beta=10\mu\text{m}$, $n_{pe}=1\times 10^{17}\text{ cm}^{-3}$).

Figure 8: Calculated energy spectra (W) as a function of frequency (ω) and solid angle (Ω).

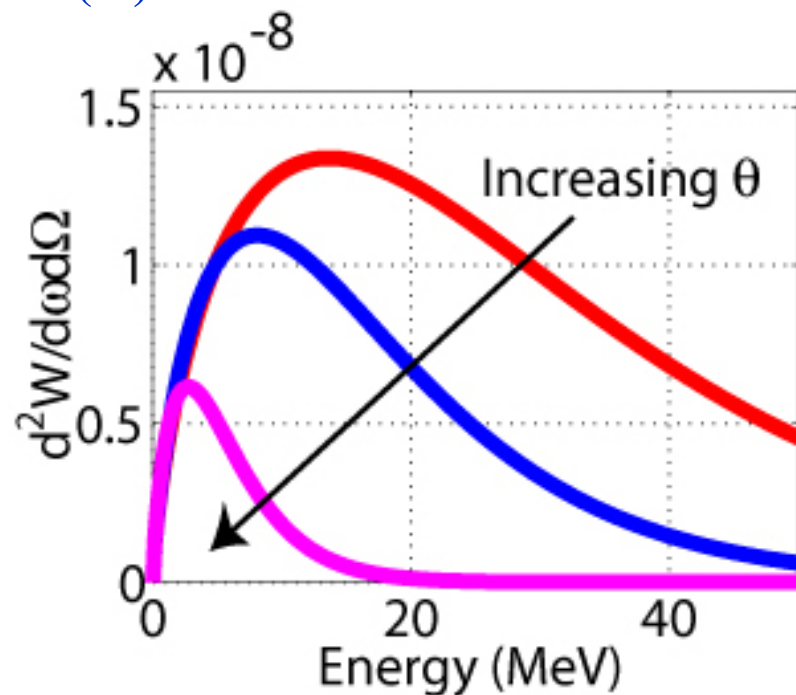
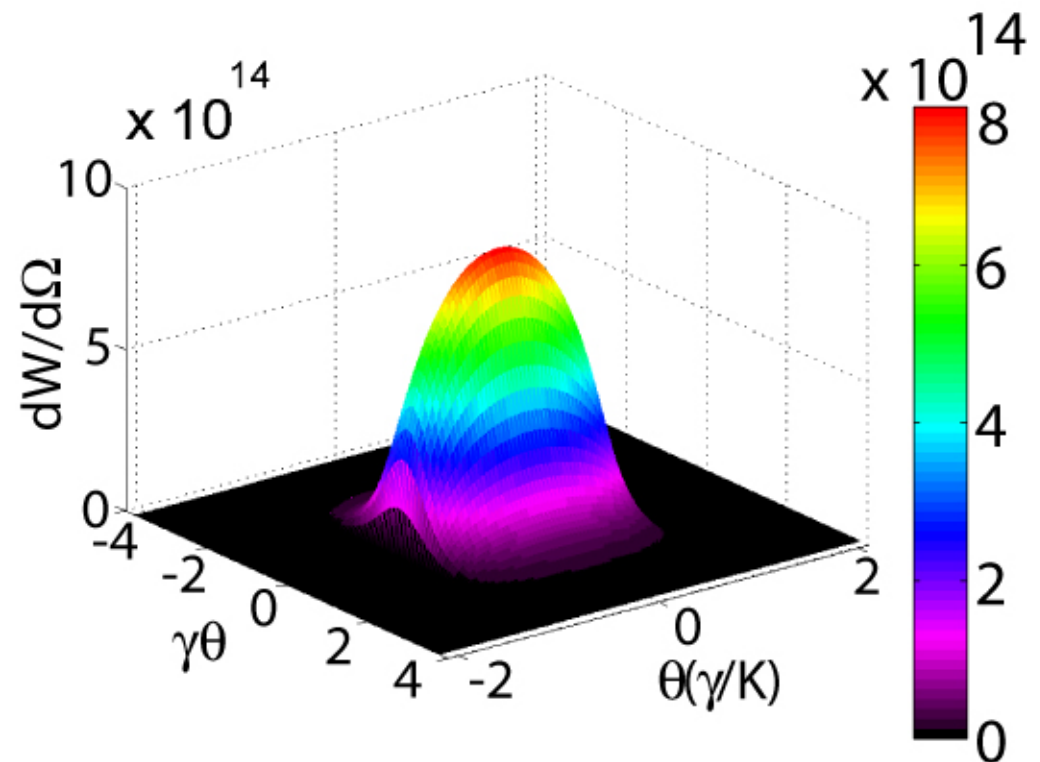


Figure 9: Calculated energy (P) as a function of solid angle (Ω).





Radiated Energy Agreement



- The Larmor Formula theoretical energy vs. Integrated calculated energy using the Saddle-Point Method

Larmor Formula Energy Loss Equation:

$$\frac{dE}{dz} = \frac{1}{3} r_e m_e c^2 \gamma^2 k_\beta^2 K^2 = f(n_p^2, r_o^2, \gamma^2)$$

Table 2: Error Between Larmor Theory and Saddle-Point Calculation

<i>Plasma Density (n_{pe})</i>	<i>Larmor Formula (MeV)</i>	<i>Calculated Saddle-Point (MeV)</i>	<i>% Error</i>
1×10^{17}	66.5	66.0	0.752
2×10^{17}	188.1	187.8	0.159
3×10^{17}	346	348	0.578
1×10^{17} Gaussian	1.307×10^{12}	1.315×10^{12}	0.605



Electron-Gamma Shower Code (EGS4)



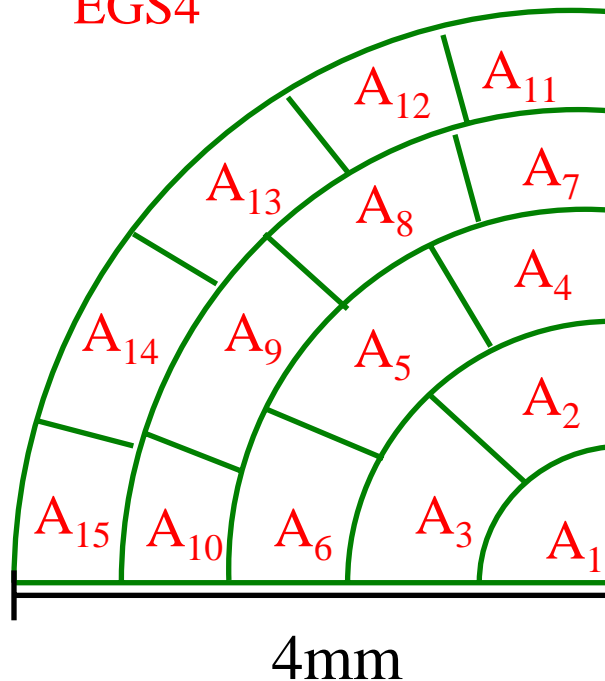
UCLA



- EGS4 is a Monte Carlo simulation package for the transport of photons and charged particles with keV to TeV energies through arbitrary geometry targets

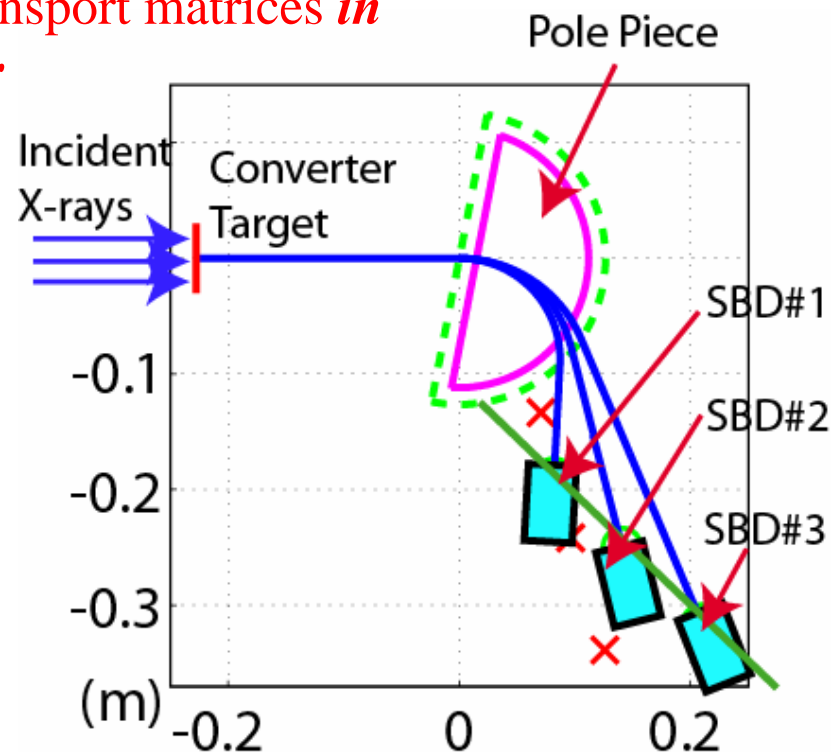
Figure 10: EGS4 code for virtual positron detection

1) X-ray collide with the segmented converter target in EGS4



2) Outgoing e^+ sent through magnetic transport matrices *in air*

3) e^+ detected by virtual SBD





Simulation Parameters



- There are 3 input parameters for calculating the spectrum.
 - 1) N_{bi} - beam electrons radiating in the ion column
(N_b - *total* number of beam electrons)
 - 2) γ_{bi} - energy of the beam electrons (i.e. the wake losses)
(γ_b - *incident* electron beam energy)
 - 3) $\sigma_{i;x,y}$ - the rms radius of the electron beam within the peak density region of the plasma (ramped-density focusing)
($\sigma_{x,y}$ - *vacuum* electron beam spot size)

- *Using the linac parameters (i.e. $N_b, \gamma_b, \sigma_{x,y}$), the e^+ yield calculation is off by a factor of ~ 30 .*

- *How are these values calculated?*

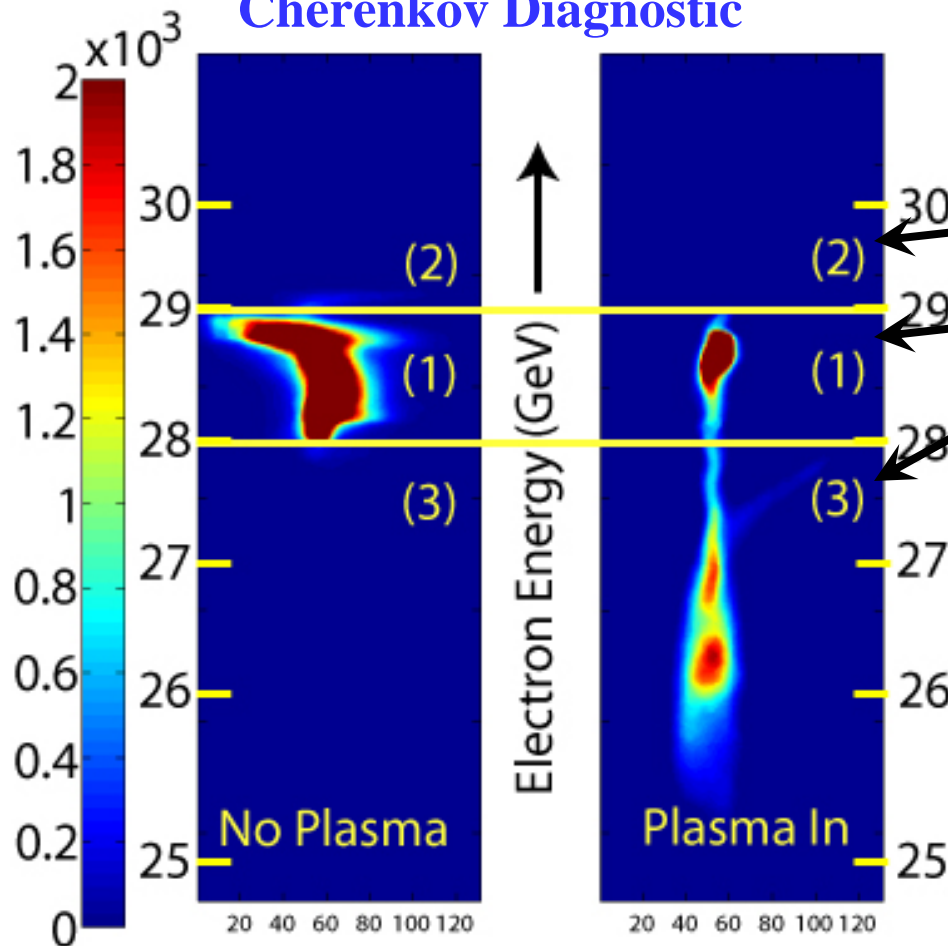


Estimate of γ_{bi} and N_{bi}



- The spectrometer images are used to estimate N_{bi} .
- *Postulate: For our regime, N_{bi} is the number of electrons that lose energy.*

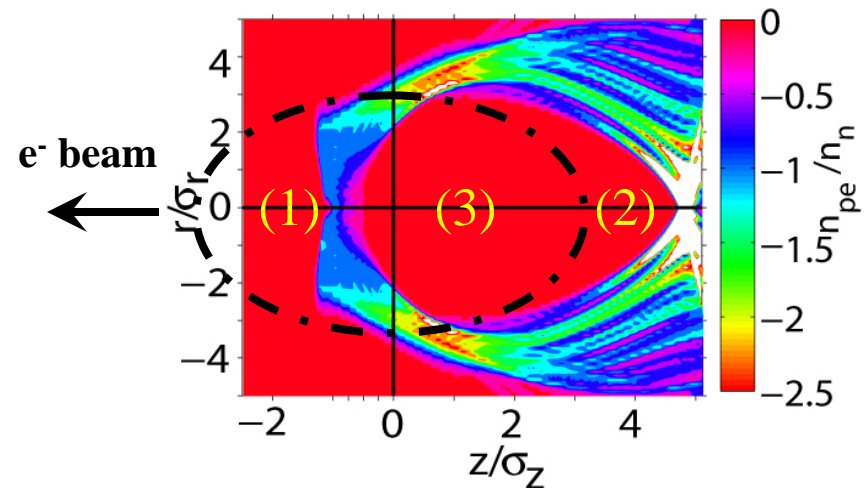
Figure 11: Typical images from the Cherenkov Diagnostic



How is it determined:

- Split energy spectrum of beam e^- into 3 regions:

- 2) *Energy Gain Region*
- 1) *Unaffected Region*
- 3) *Energy Loss Region*





Estimate of γ_{bi} and N_{bi} (cont.)



- 50% charge point in region (3) will give us the mean energy loss.

Figure 12: Cherenkov Diagnostic Image

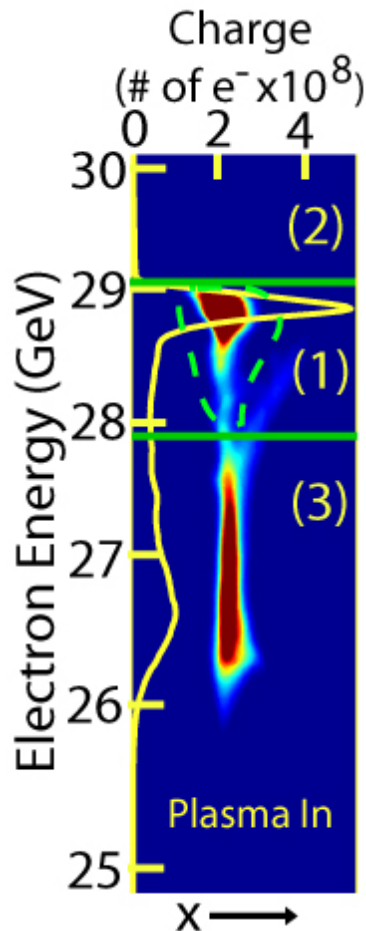


Figure 13: Measured Ion Column Charge (N_{bi})

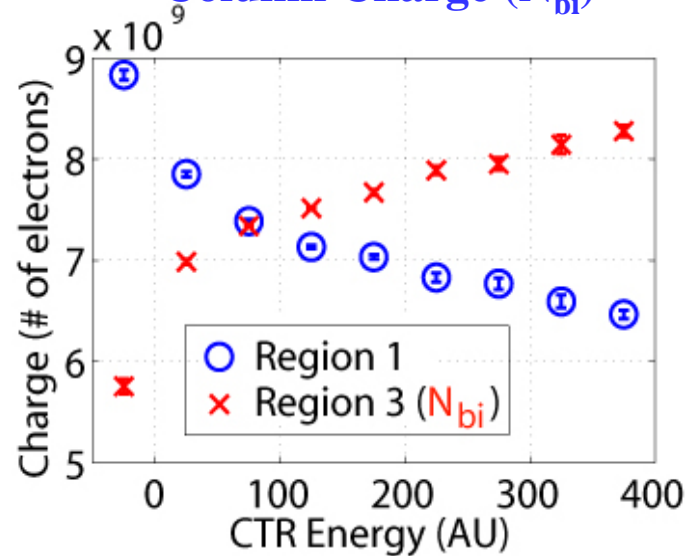


Figure 14: Measured Ion Column Wakeloss

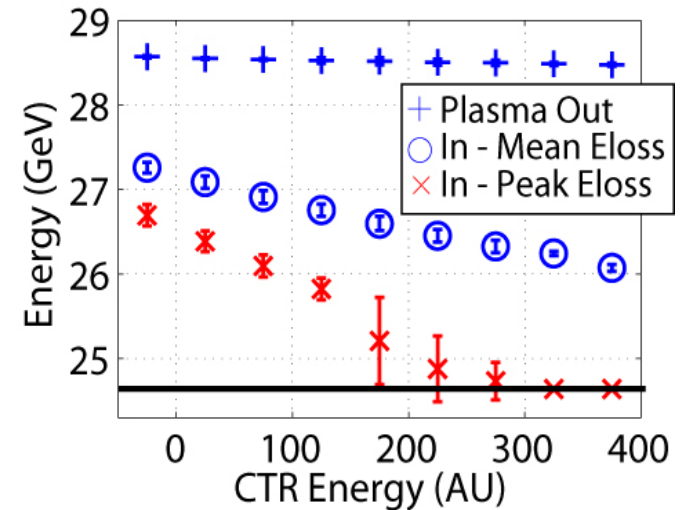
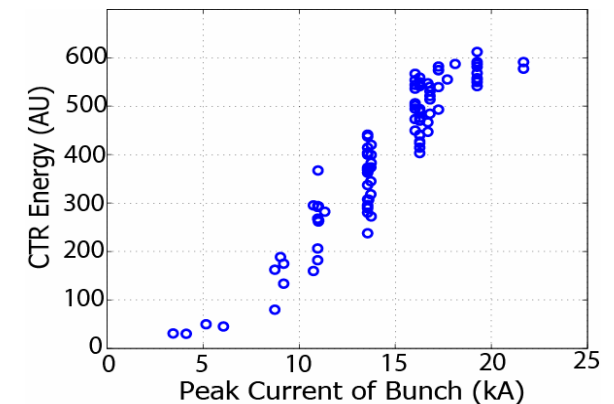


Figure 15: CTR versus Peak Beam Current ($\sim 1/\sigma_z$)
C.D. Barnes, Ph.D, Stanford (2006).





Estimation of the rms radius of the beam envelope inside the plasma: $\sigma_{i:x,y}$



UCLA



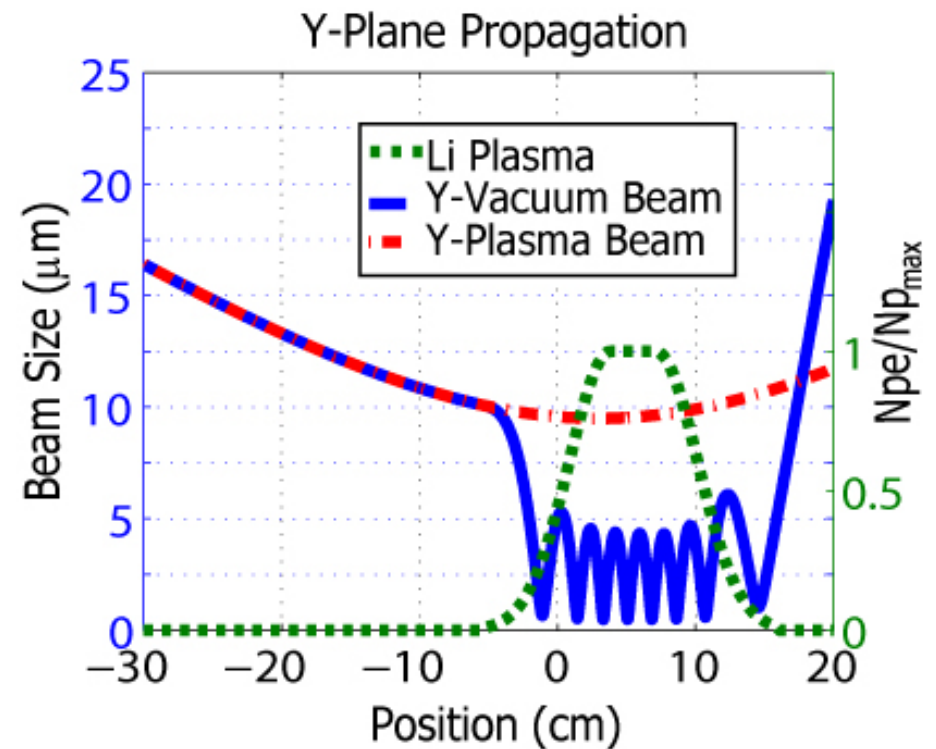
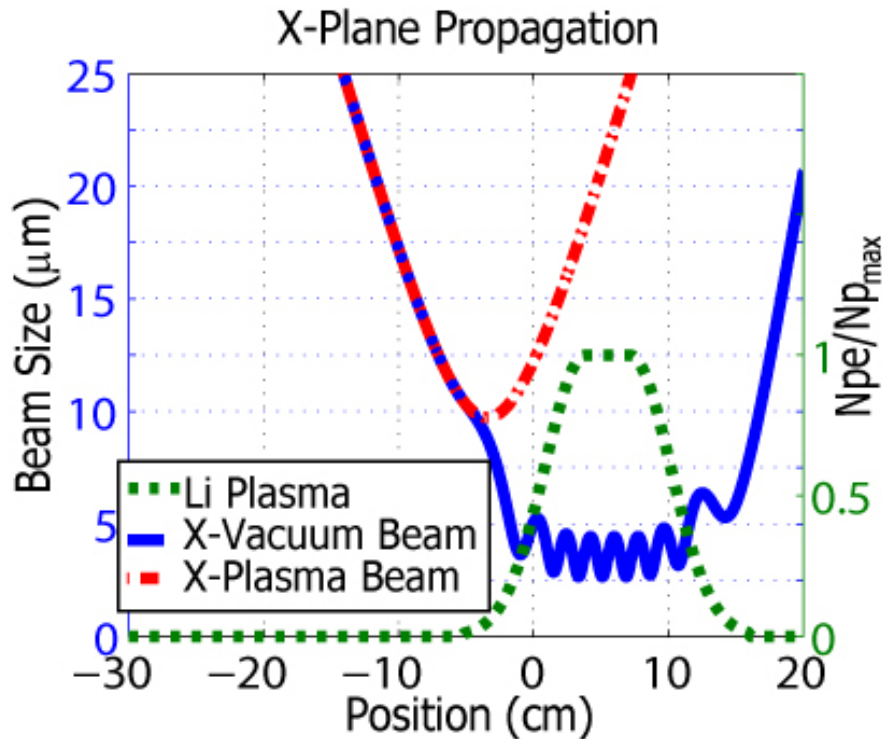
- Compute using the beam envelope equation with the linac beam parameters

$$\frac{d^2 \sigma_{x,y}(z)}{dz^2} + \left[k_\beta^2 - \frac{\epsilon_{N:x,y}^2}{\gamma^2 \sigma_{x,y}^4(z)} \right] \sigma_{x,y}(z) = 0$$

- Assumes a full ion column

Figure 16: X-Plane propagation with ramped-density plasma ($\sigma_{i:x}=4\mu\text{m}$) ($n_{pe:\text{max}}=1 \times 10^{17} \text{ cm}^{-3}$).

Figure 17: Y-Plane propagation with ramped-density plasma ($\sigma_{i:y}=4\mu\text{m}$).

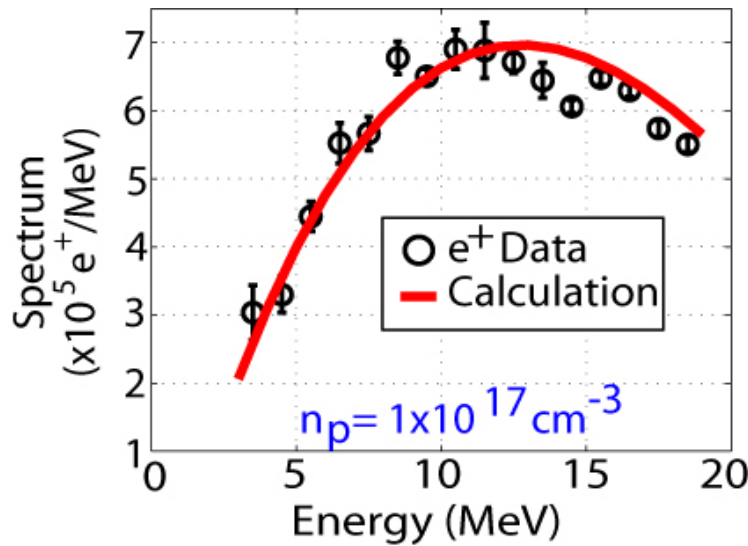




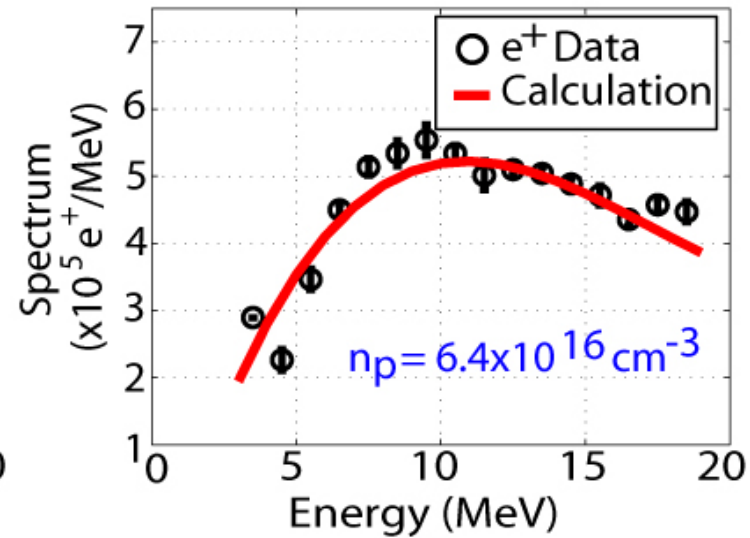
Positron Spectra at 3 Different Densities



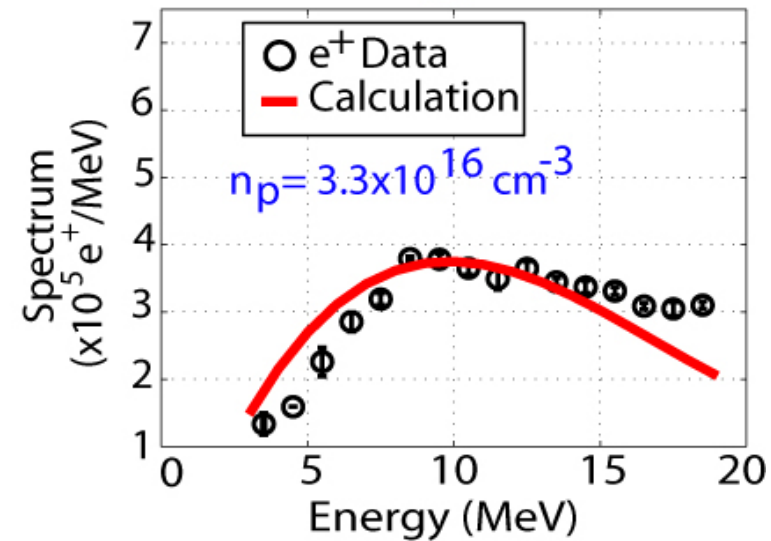
UCLA



(a)



(b)



(c)

Figure 18: Measured and calculated positron spectra for the 3 cases quoted in Table 3.



Positron Yield Vs. Density



- Each case has a different N_{bi} , γ_b , and $\sigma_{i;x,y}$ giving a very different scaling than n_{pe}^2

Figure 19: Measured and Calculated positron yields versus density for the 3 cases shown on the previous slide.

Variation is $\sigma_{x,y} = \pm 0.5 \mu\text{m}$.

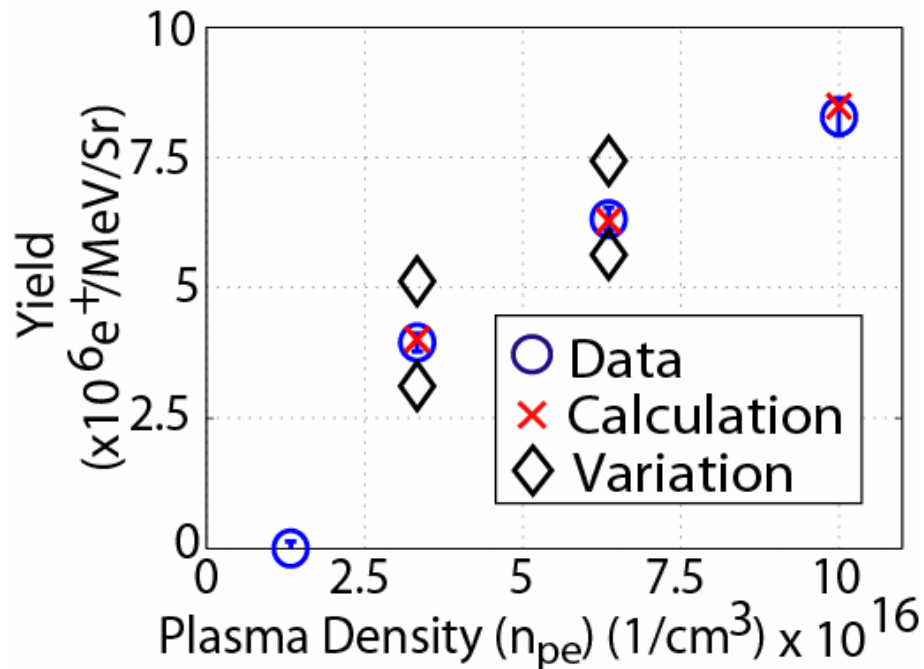
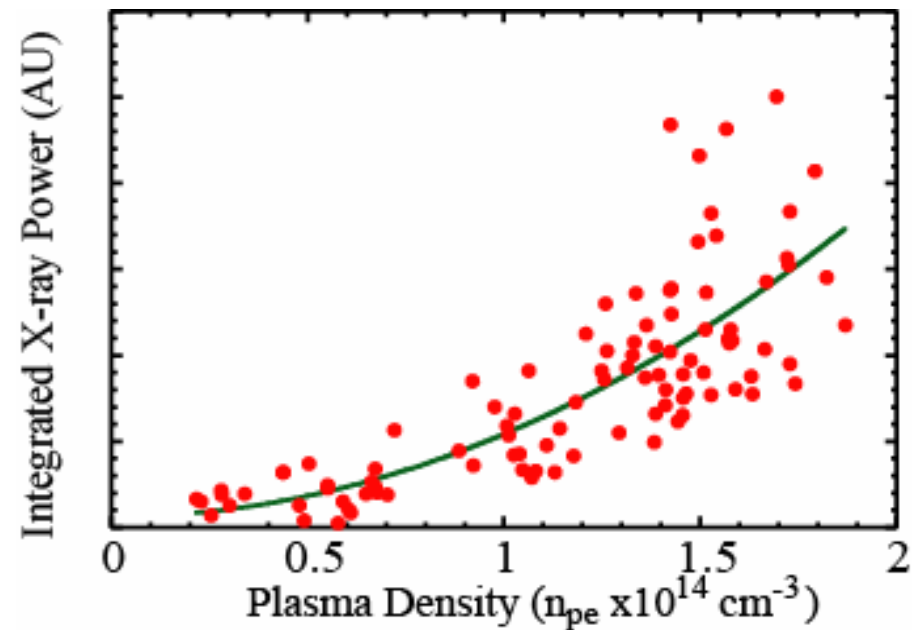


Figure 20: Total measured X-ray power vs. the plasma density shown in Figure 2 for $n_{pe} = 1 \times 10^{14} \text{ cm}^{-3}$.



S. Wang et al. Phys. Rev. Lett. Vol 88. Num 13, pg. 135004, (2002)



Positron Yield Vs. CTR Energy



- CTR energy has a large effect on N_{bi} and γ_b ,
- It should also have an effect on the positron yield.
- Positron yield peaks near CTR of 200.

Figure 21: Measured Ion Column Charge (N_{bi}) using the Cherenkov diagnostic.

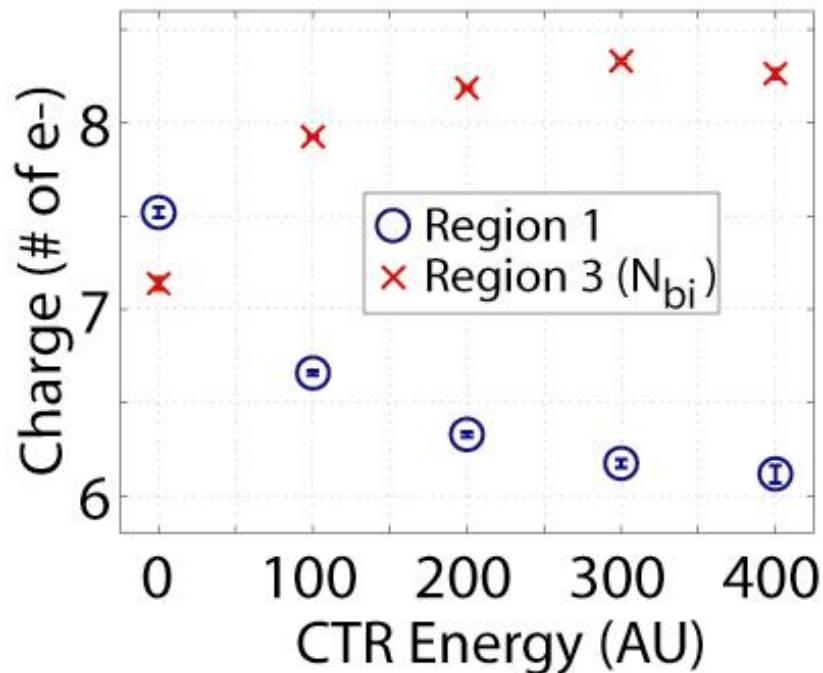
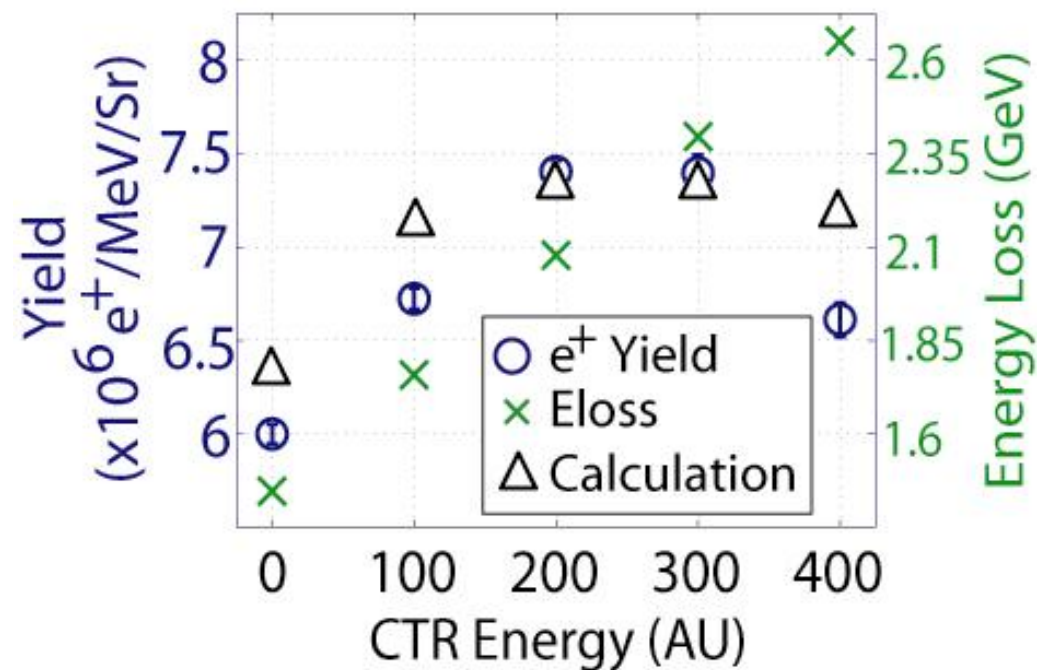


Figure 22: Measured Positron Yield versus CTR. Also plotted is the Mean and Peak Energy Loss using the Cherenkov diagnostic





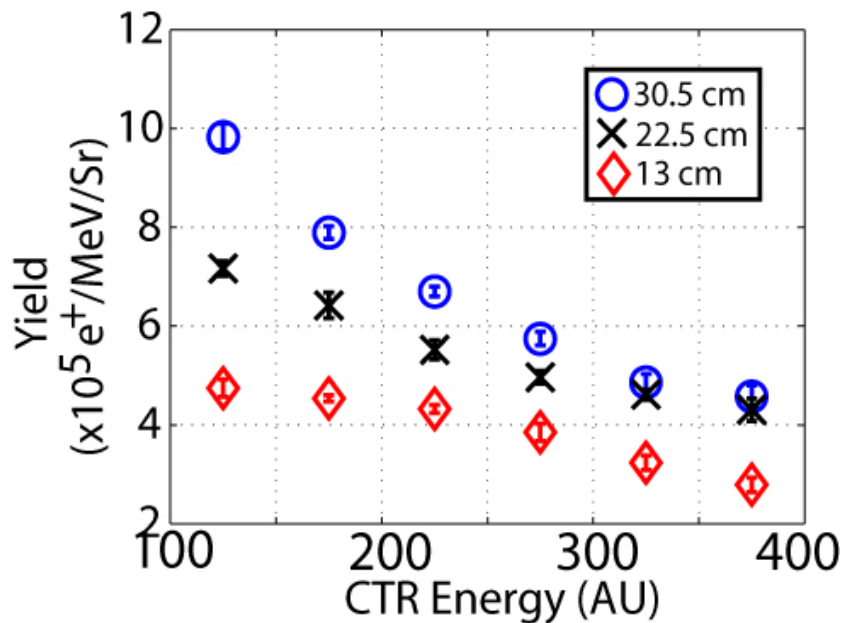
Positron Yield Vs. Plasma Length



- The positron yield as a function of plasma length with $n_{pe}=2.7 \times 10^{17} \text{ cm}^{-3}$ for the 27-30 MeV positron energy bin.

Figure 23: Integrated Positron Yield from 27-30 MeV for $n_{pe}=2.7 \times 10^{17} \text{ cm}^{-3}$ versus CTR energy for three different plasma lengths.

Table 4: Estimated and Measured relative yields for the 175 CTR bin in figure 29.



Case	1	2	3
Plasma Length (cm)	13	22.5	30.5
Wakeloss (GeV)	3.1	3.8	4.7
Average Beam Energy (GeV)	26.95	26.6	26.15
Estimated e ⁺ Yield	1.0	1.55	1.97
Measured e ⁺ Yield	1.0	1.47	1.87



Conclusions



- 1) Positron have been created and measured using MeV X-rays emitted from electron betatron motion in a plasma.
- 2) Positron spectra have been measured as a function of plasma density, wakeloss and plasma length
- 3) The agreement between the computed spectra and the measured spectra is excellent.
- 4) Given our agreement, we are confident that we can use this model to design a potential positron source for a linear collider. Using the following parameters:
 - $E_{\text{beam}}=50 \text{ GeV}$, $N_b=4 \times 10^{10}$, $N_p=3 \times 10^{17} \text{ cm}^{-3}$, $\sigma_{x,y}=9 \mu\text{m}$, $\sigma_z=35 \mu\text{m}$, $L_p=1 \text{ m}$

Result: 0.44 e^+/e^-



UCLA





Positron Detection Null Tests



- Initial test performed to convince ourselves that the signal was from the converter target.

Table 1: Relative scaling for different positron data tests

Plasma	Positron Target	Magnet	Signal (AU)
OUT	OUT	OFF	1
OUT	OUT	ON	1
OUT	IN	OFF	1
OUT	IN	ON	1
IN	OUT	OFF	50
IN	IN	OFF	50
IN	OUT	ON	300
IN	IN	ON	2000

NOTE: Magnet “on” assumes 10 MeV positron detection



Lithium Plasma Source



UCLA

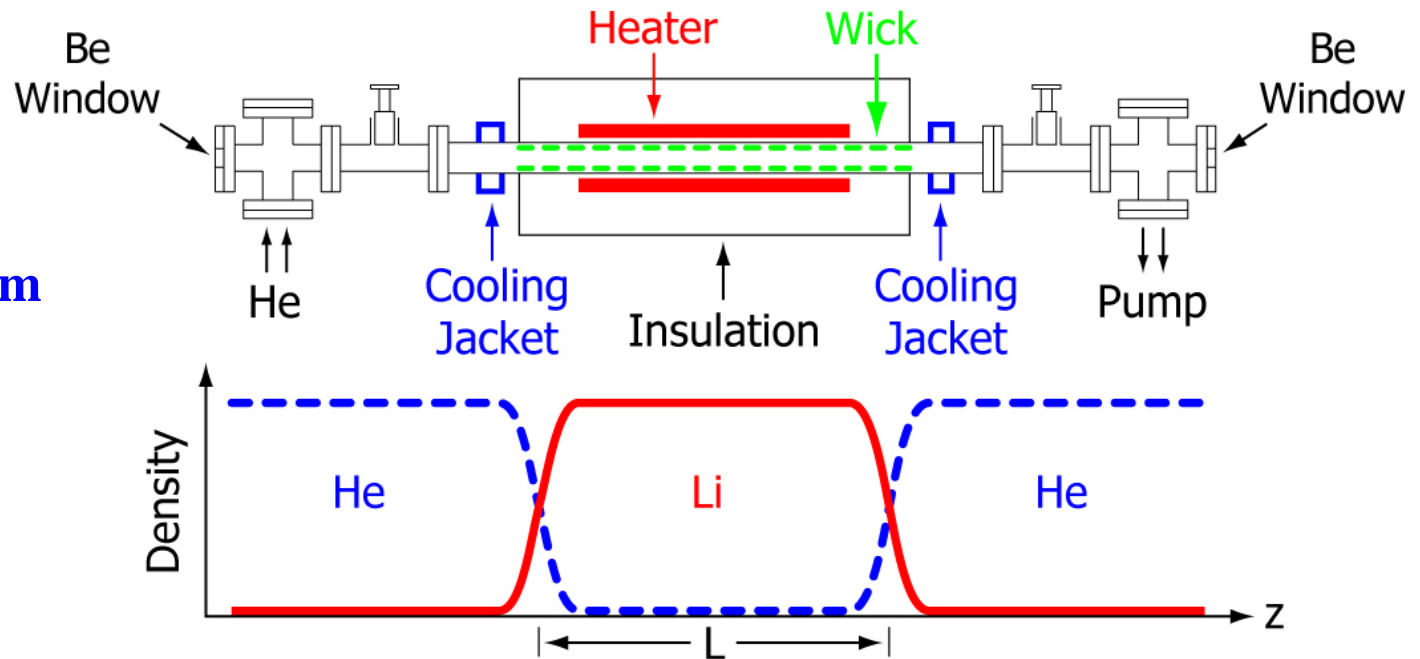


Figure 4: Lithium Oven Diagram

How it works:

- 1) Heated to 800°C to vaporize solid Li.
 - 2) Li vapor diffuses out to the He transition region and condenses on wick.
 - 3) The molten Li wicks back to center, vaporizes and begins the process again.
- Be (low-Z) windows separate the He from the FFTB beam line vacuum.
 - The He pressure determines the Li vapor density, and the heater power determines the Li vapor length



Field Ionization

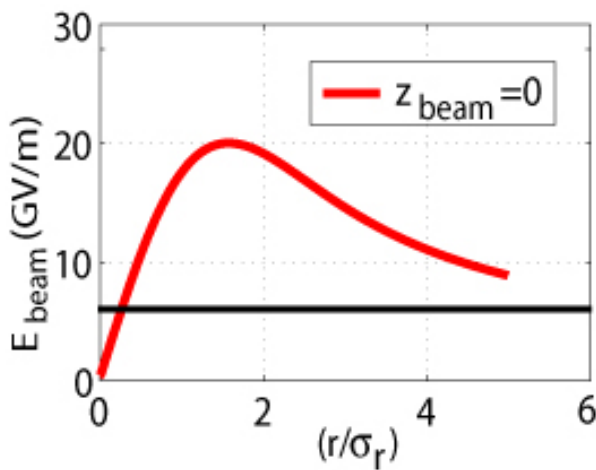


Figure 5: E_r of a Gaussian beam ($\sigma_r=11\mu\text{m}$, $\sigma_z=29\mu\text{m}$).

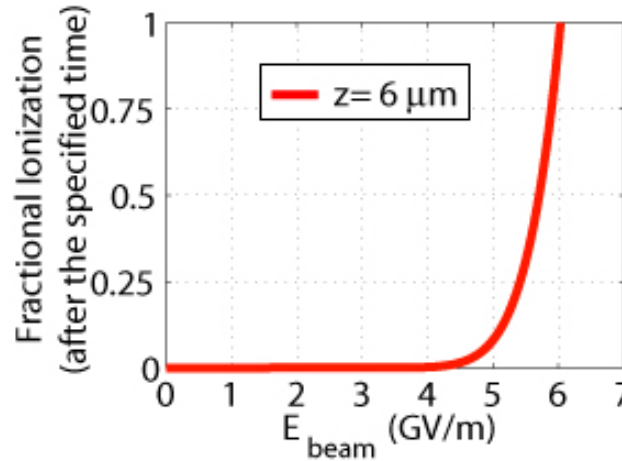


Figure 6: The fractional ionization of Li atoms (20 fs).

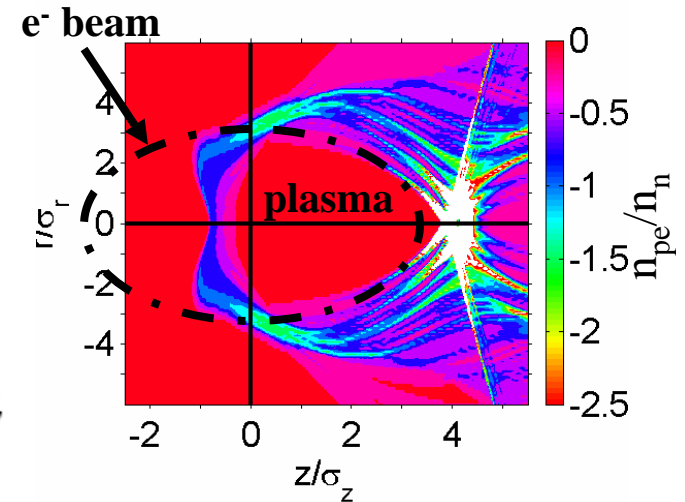


Figure 7: QuickPIC simulation of n_{pe} contours with $n_n=1 \times 10^{17} \text{ cm}^{-3}$ with Gaussian beam ($\sigma_r=11\mu\text{m}$, $\sigma_z=29\mu\text{m}$).

- Li vapor ionizes when $E_{r,beam} > 6 \text{ GV/m}$ (Figure 6).
- Ionization is fast ($\sim 20 \text{ fs}$) (Figure 7).
- The full ion column begins roughly at the longitudinal center of the electron beam (black dashed line) (Figure 8).

C O'Connell
Ph.D, Stanford
(2005)



Radiated Energy Agreement



- The following table is a chart of the Larmor Formula theoretical energy vs. Integrated calculated energy using the Saddle-Point Method

Table 1: Error Between Larmor Theory and Saddle-Point Calculation

<i>Plasma Density (n_{pe})</i>	<i>Larmor Formula (MeV)</i>	<i>Calculated Saddle- Point (MeV)</i>	<i>% Error</i>
1×10^{17}	66.5	66.0	0.752
2×10^{17}	188.1	187.8	0.159
3×10^{17}	346	348	0.578
1×10^{17} Gaussian	1.307×10^{12}	1.315×10^{12}	0.605

- Integral is performed in the following steps.
 - Calculate the Lienard-Wiechert Potential $\frac{\partial^2 W}{\partial \omega \partial \Omega}$
 - Integrate over frequency at each position $\frac{\partial P(\theta, \phi)}{\partial \Omega} = \int \frac{\partial^2 W(\omega, \theta, \phi)}{\partial \omega \partial \Omega} \partial \omega$
 - Integrate over solid angle $E = \int \frac{\partial P(\theta, \phi)}{\partial \Omega} \partial \Omega$

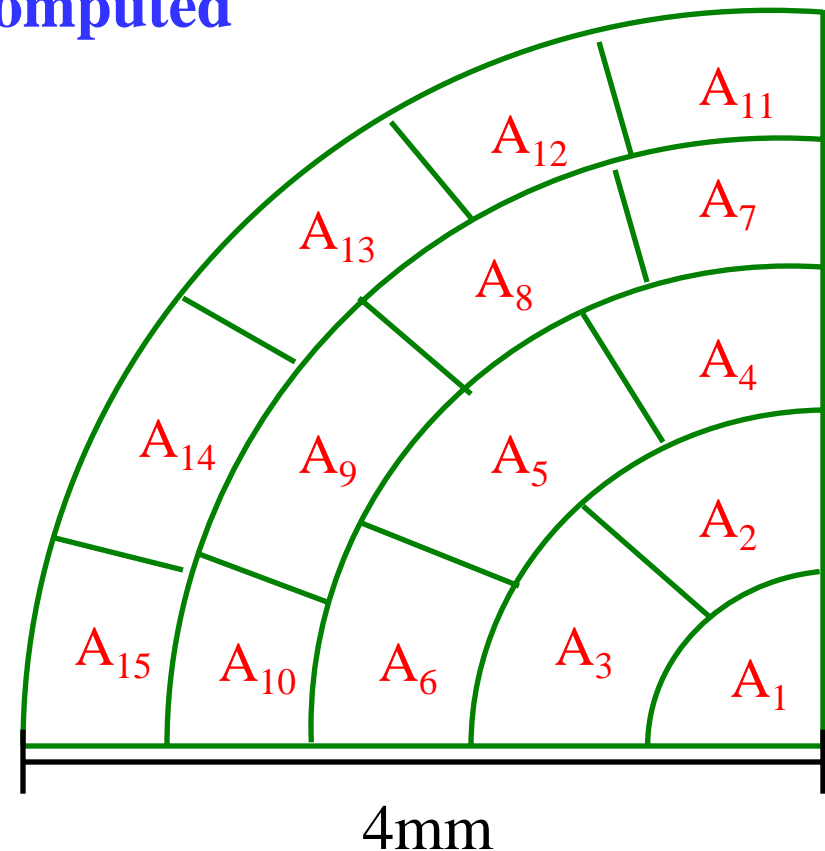


Electron-Gamma Shower Code (EGS4)



- EGS4 is a Monte Carlo simulation package for the transport of photons and charged particles with keV to TeV energies through arbitrary geometry targets
 - 1) Split the quadrant into 15 areas
 - 2) Compute the spectral distribution and the total energy in each area.
 - 3) Use the spectral distribution and total energy to get the number of photons/energy in each bin.
 - 4) Normalize the spectral distribution by the total number of photons in the area -> ***Input into EGS4 input deck***
 - 5) Compute the Center of Each Area -> ***Input into EGS4 input deck!***
 - 6) After the target, positrons are propagated in EGS4 through the proper magnetic transport matrices in air to account for air scattering to the detectors.

Figure 15: 2nd quadrant of Far-field where radiation spectrum is computed





1) N_{bi} – Electrons in Ion Column

- The images from the Cherenkov energy diagnostic determine this value.

Figure 16: (a) Typical plasma “out” shot (b) Typical plasma “in” shot on the Cherenkov Diagnostic

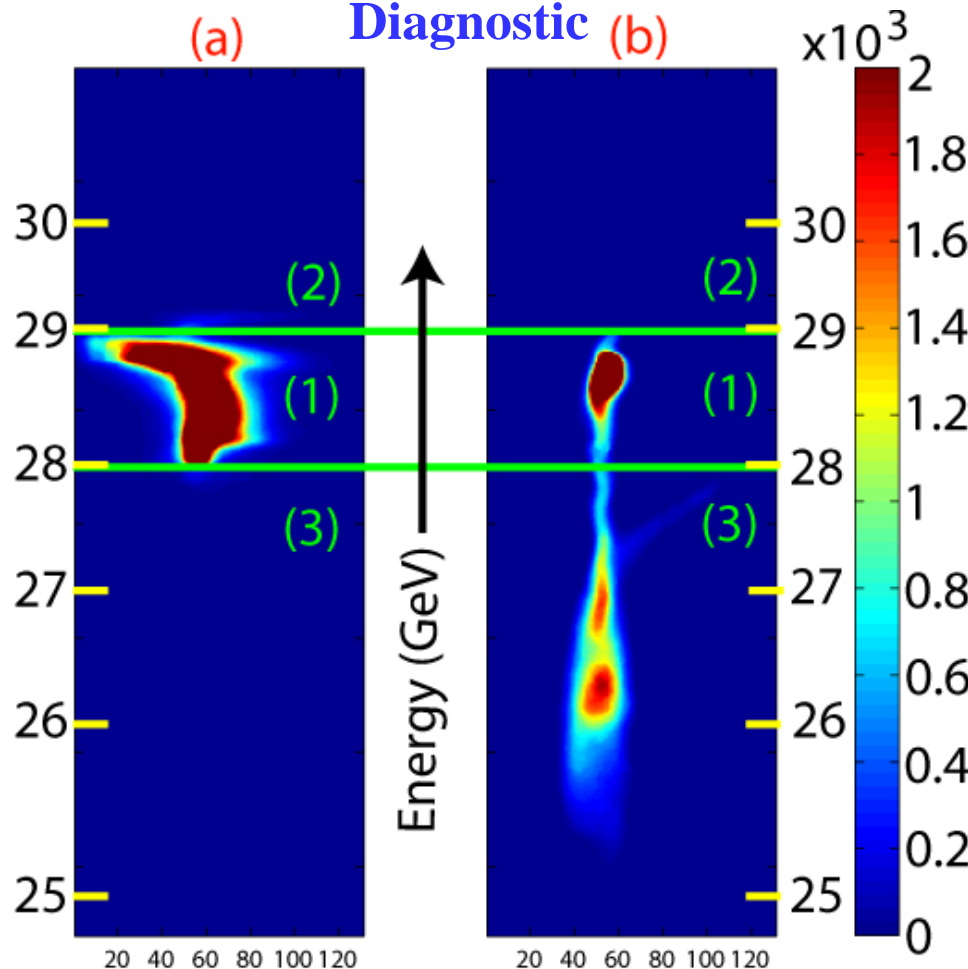
N_{bi} is determined as the number of electrons that lose energy.

We need 3 things:

- 1) A background shot for subtraction
- 2) The total number of counts on the 16-bit camera in the ROI (charge/count) (Plasma Out)
- 3) Split Plasma IN case into 3 regions:
 - 1) *Unaffected Region*
 - 2) *Energy Gain Region*
 - 3) *Energy Loss Region*

Procedure:

- 1) **Sum the counts in each region (1), (2), and (3).**
- 2) **Multiply by the charge/count calibration to get the number of electrons in each region.**
- 3) **N_{bi} is defined as the electrons in region (3) for these beam parameters.**





N_{bi} accuracy?



- This simulation was performed by matching the peak energy loss in QuickPIC with that measured on the Cherenkov diagnostic.
- Only 1.4 % of N_b is in the accelerating wake. Thus, N_{bi} is the number of electrons losing energy as measured on the Cherenkov images in the experiment.

Figure 17: QuickPIC simulation plotting n_{pe} contours versus longitudinal position with a $N_b=1.2 \times 10^{10}$ Gaussian beam with $\sigma_r=11 \mu\text{m}$ and $\sigma_z=22.5 \mu\text{m}$ in an $n_{pe}=1 \times 10^{17} \text{ cm}^{-3}$ plasma.

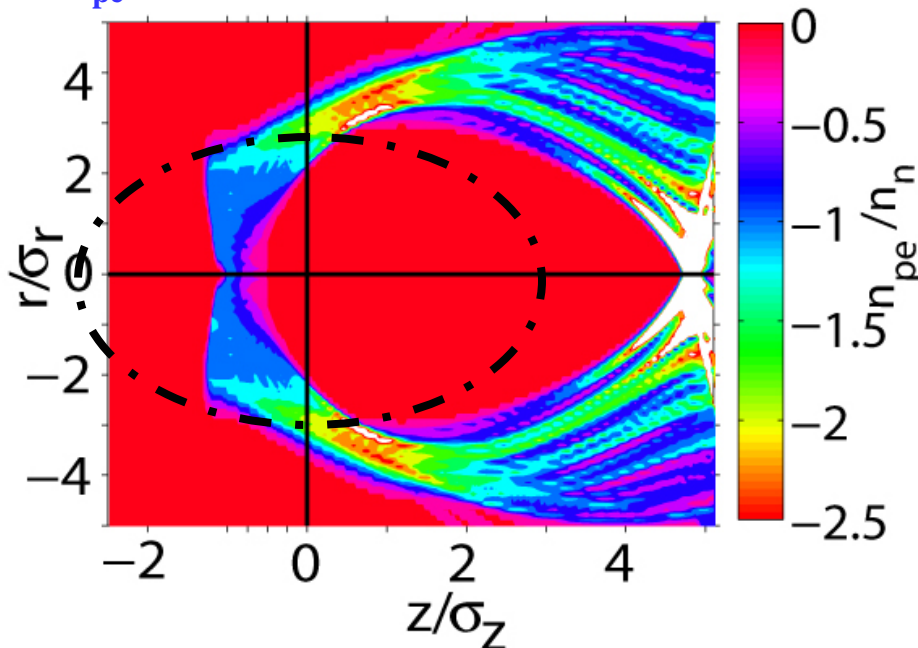
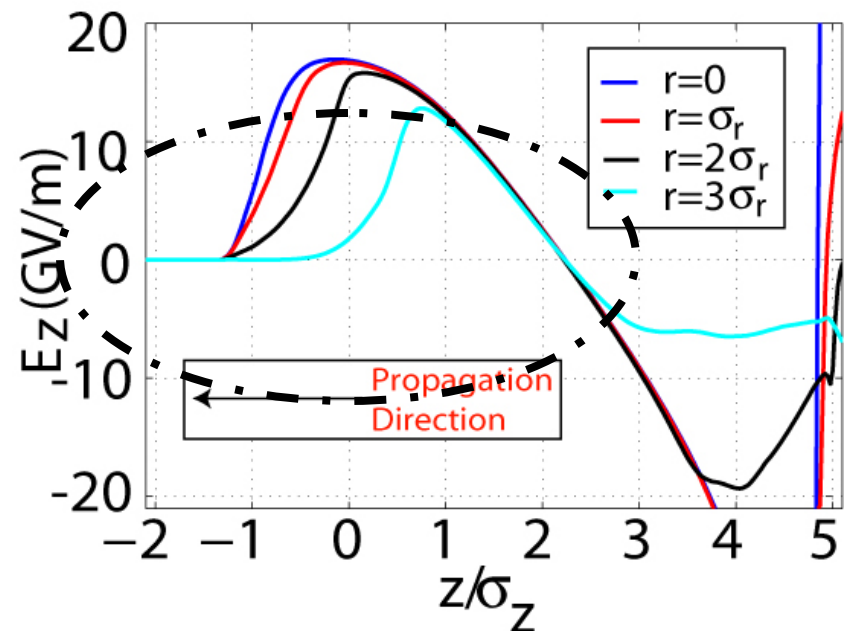


Figure 18: QuickPIC simulation plotting E_z (longitudinal wakefield) for various radial positions versus longitudinal position for the same beam as in figure 17.

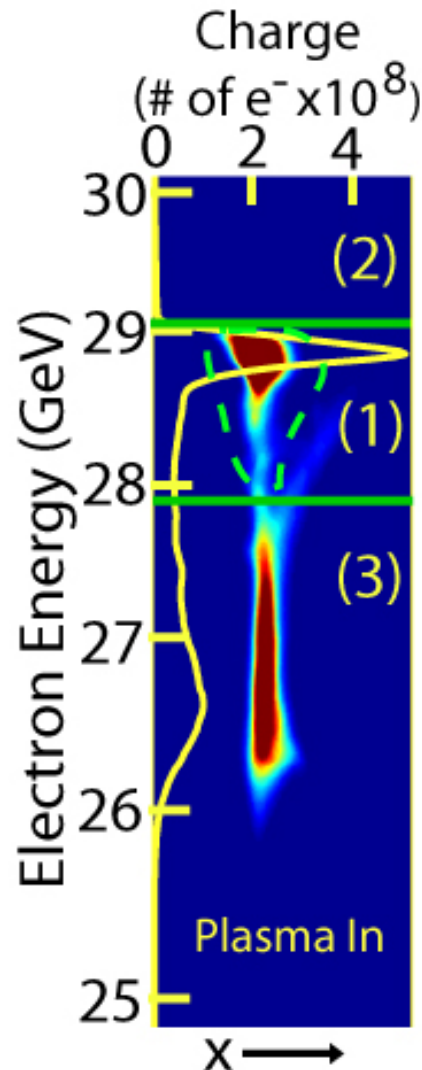




2) Estimate of γ_{bi} and N_{bi} (cont.)

- Again, the Cherenkov images are used to determine this value.

Figure 19: Typical image from Cherenkov Diagnostic



The beam energy loss will decrease the X-ray yield due to the γ_{bi}^2 dependence on electron radiated energy.

A) 50% charge point in region (3) will give us the mean energy loss.

Procedure:

- 1) For all energy pixels, sum in “x”. This will give the charge distribution as a function of energy (yellow line).
- 2) Determine the total charge in region (3) from the charge (*plasma “out”-region (2)- region (1)*).
- 3) Integrate down over the energy pixels beginning from the green line at 27.9 GeV until 50% of the charge in region (3) is reached.
- 4) This is the mean energy loss which is inputted into the code.



3) $\sigma_{i:x,y}$ – Rms Radius of the Radiating Electrons

- Compute using the beam envelope equation with the linac beam parameters.

1) Measure emittance at the end of the linac ($\epsilon_{o:x,y}$)

2) Measure OTR size (σ_x, σ_y)

3) Measure Waist location using the size on OTR 1 and 2.

4) Compute emittance at the waist location

$$\epsilon_{x,y}^2 = \epsilon_{o:x,y}^2 + \sigma_{x,y}^2 \left[\theta_{Be}^2 + \theta_{Ti}^2 \right]$$

5) Values give the waist position and size in vacuum.

6) Put in the plasma profile and solve.

Figure 21: X-Plane propagation with ramped-density plasma focusing ($n_{pe:max}=1 \times 10^{17} \text{ cm}^{-3}$) giving $\sigma_{i:x}=4 \mu\text{m}$.

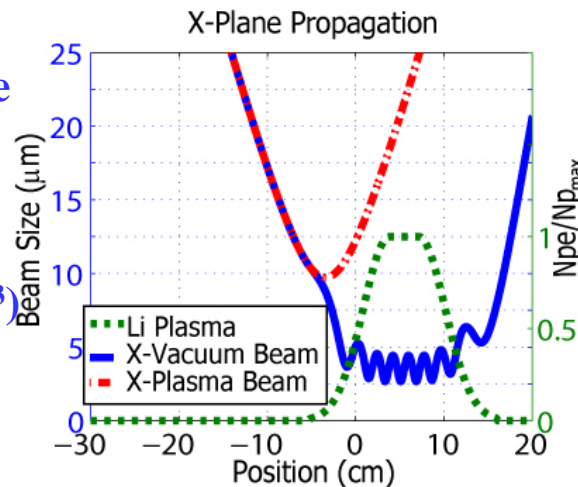
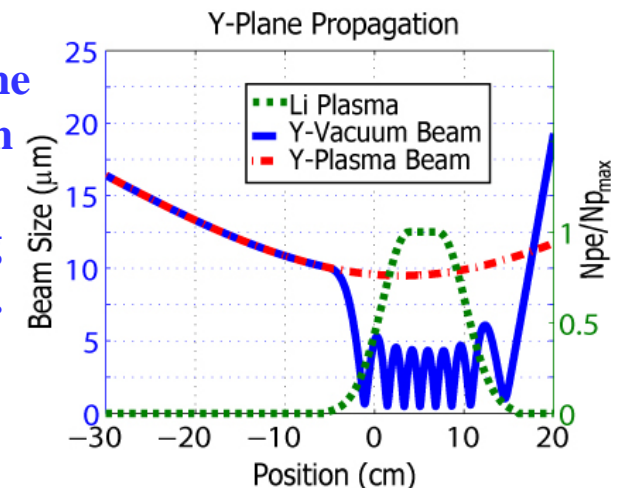


Figure 22: Y-Plane propagation with ramped-density plasma focusing giving $\sigma_{i:y}=4 \mu\text{m}$.





Parameters Vs. CTR Energy



- Upstream of the plasma, the CTR of the electron beam is measured as the beam traverses a $1\mu\text{m}$ Ti foil, scaling as $1/\sigma_z$. The wakeloss also has a σ_z scaling.
- The conversion to σ_z for this data was not necessary because the wakeloss was an experimentally measured quantity whereas the conversion to σ_z was computed.
- However, CTR energy had a large effect on N_{bi} and γ_b , and can help us to observe scaling laws.

Figure 26: Measured Ion Column Charge (N_{bi}) using region (3) “Energy Loss” and region (1) “unaffected” on the Cherenkov Diagnostic.

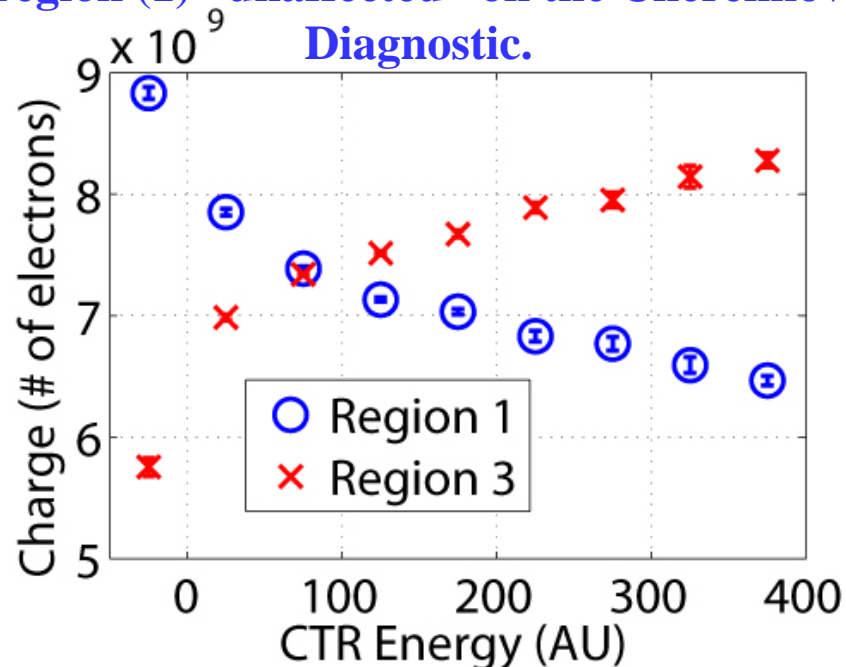
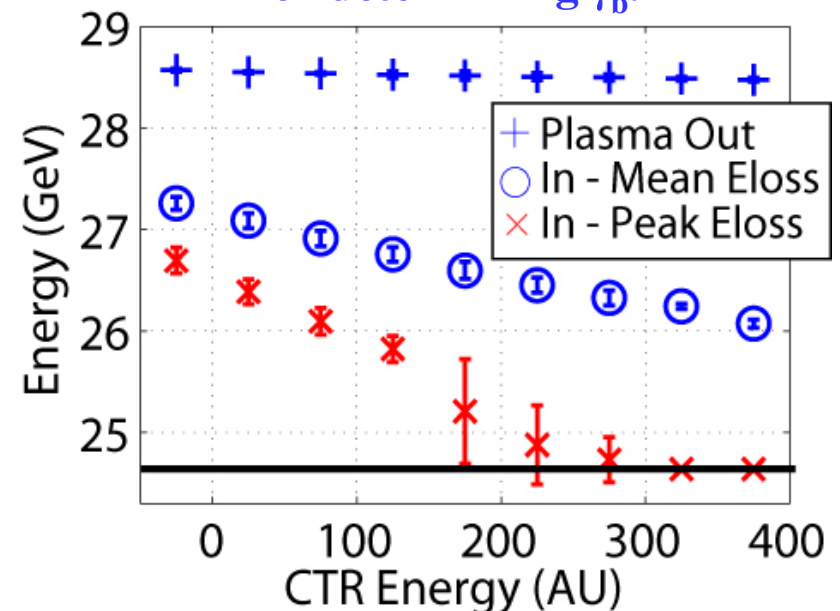


Figure 27: Measured Mean and Peak Energy Loss in region (3) “Energy Loss” for the $n_{pe}=1 \times 10^{17} \text{ cm}^{-3}$ case for determining γ_b .





Positron Yield Vs. Plasma Length



- We were able to compute the positron yield as a function of plasma length with $n_{pe}=2.7 \times 10^{17} \text{ cm}^{-3}$ for the 27-30 MeV positron energy bin.

Figure 29: Integrated Positron Yield from 27-30 MeV for $n_{pe}=2.7 \times 10^{17} \text{ cm}^{-3}$ versus CTR energy for three different plasma lengths.

- Yield increases with length as expected, but saturates at high CTR energies (wakefields) at the 22.5 and 30.5 cm lengths (γ_b^2 dependence).
- Although we could not measure the energy loss for all CTR bins (energy spread too large), we did have a value for the CTR=175 bin, estimated yield:

- Case 1: $26.95^2 \text{ [GeV}^2] * (13+3) \text{ [cm]} = 11621 \text{ AU}$
- Case 2: $26.60^2 \text{ [GeV}^2] * (22.5+3) \text{ [cm]} = 18403 \text{ AU}$
- Case 3: $26.15^2 \text{ [GeV}^2] * (30.5+3) \text{ [cm]} = 22908 \text{ AU}$

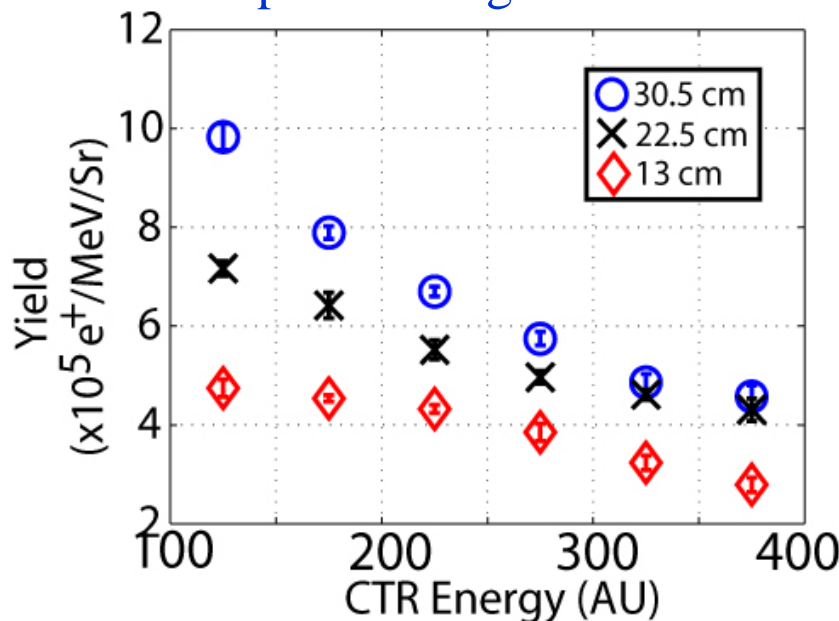


Table 3: Estimated and Measured Relative yields for the 175 CTR bin in figure 29.

Case	1	2	3
Plasma Length (cm)	13	22.5	30.5
Wakeloss (GeV)	3.1	3.8	4.7
Average Beam Energy (GeV)	26.95	26.6	26.15
Estimated e ⁺ Yield	1.0	1.55	1.97
Measured e ⁺ Yield	1.0	1.47	1.87



Future Work



- A 1-m Cs plasma source with a 2 m gap downstream to extract the electrons to eliminate thermal issues.
- A 2 mm X-ray beam collides with a $0.5X_0$ W target.
- Positrons are collected 15 cm downstream in a 4 mm radius aperture (Current parameters of the SLAC collection optics).

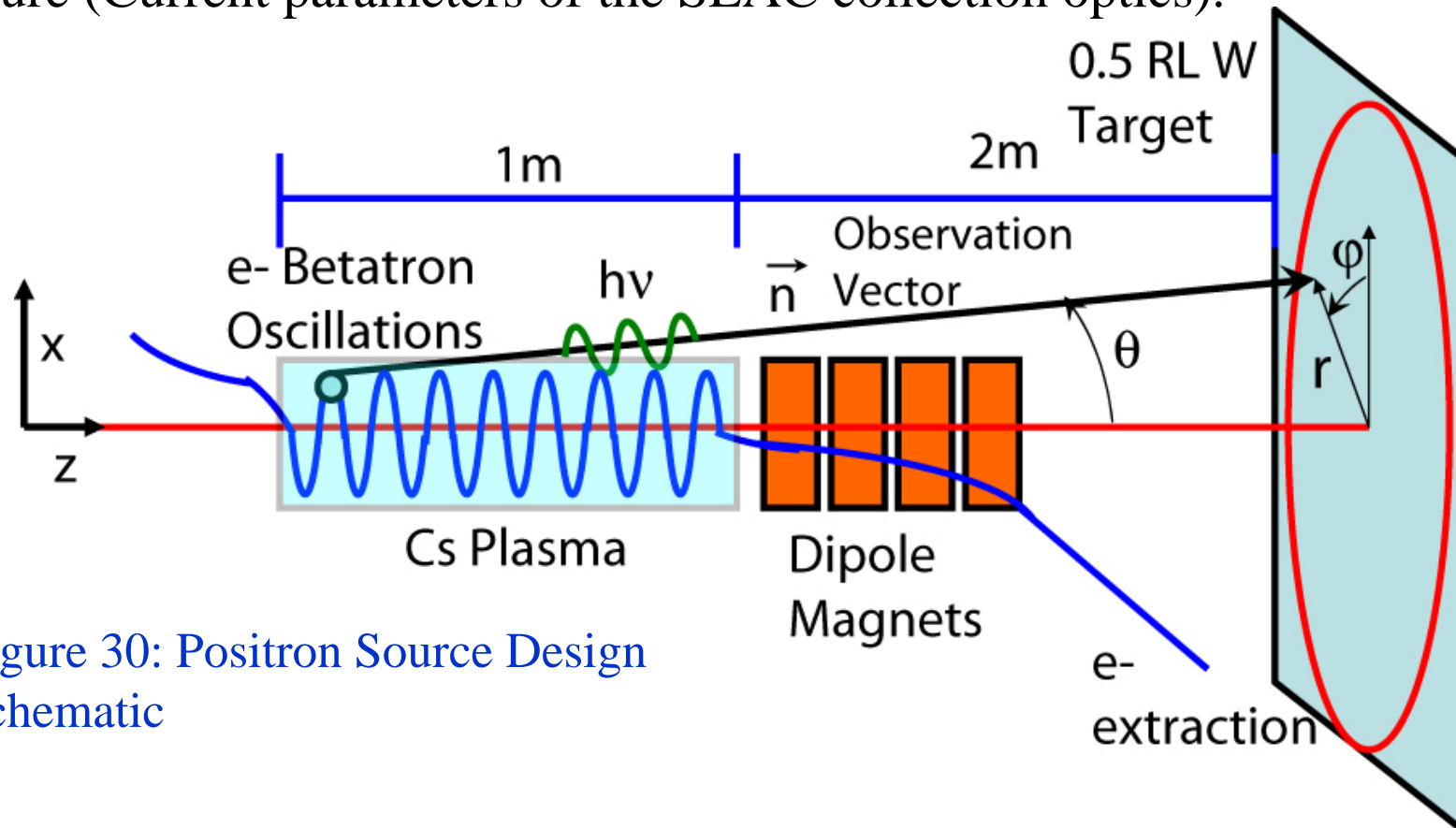


Figure 30: Positron Source Design Schematic



Source Scaling Laws



UCLA



Table 4: Determination of scaling laws in this regime using QuickPIC

<i>Parameter</i>	<i>Scaling</i>
Radiation Energy Loss (dW/dz)	$(\gamma^2, n_{pe}^2, r_\beta^2)$
Critical Energy (E_c)	$(\gamma^2, n_{pe}, r_\beta)$
Number of Photons ($[dw/dz]/E_c$)	(n_{pe}, r_β)
Maximum Ion Column Radius ($r_{i,max}$)	$(\sqrt{N_b}, 1/\sqrt{n_{pe}}, 1/\sqrt{\sigma_z})$
Peak Energy Loss ($E_{z,peak}$)	$(\sqrt{N_b}, \sqrt{n_{pe}}, 1/\sigma_z)$

- We desire:
 - 1) A small wakefield (low energy loss, large σ_z)
 - 2) However, σ_z cannot be too large since a large E_r of the beam is needed so field ionization will take place as far forward in the beam as possible, giving more N_{bi} .
 - 3) Add as many beam electrons as possible to mitigate 2).
 - 4) Also, the radius of the ion column scales as $1/\sigma_z$, dictating a need for large σ_z .
 - 4) A high n_{pe} is needed to increase the number of photons/beam e^- .
 - 5) However, a low enough n_{pe} so that as many e^- are radiating as possible (a short plasma wavelength $\lambda_\beta \sim 1/n_{pe}^{1/2}$ will decrease N_{bi}).
 - 6) A λ_β that places many beam e^- in a radiating and accelerating phase.
 - 7) A large $\sigma_{x,y}$ to radiate more X-rays, but a small enough $\sigma_{x,y}$ that will fully fit in the transverse extent of the ion column.



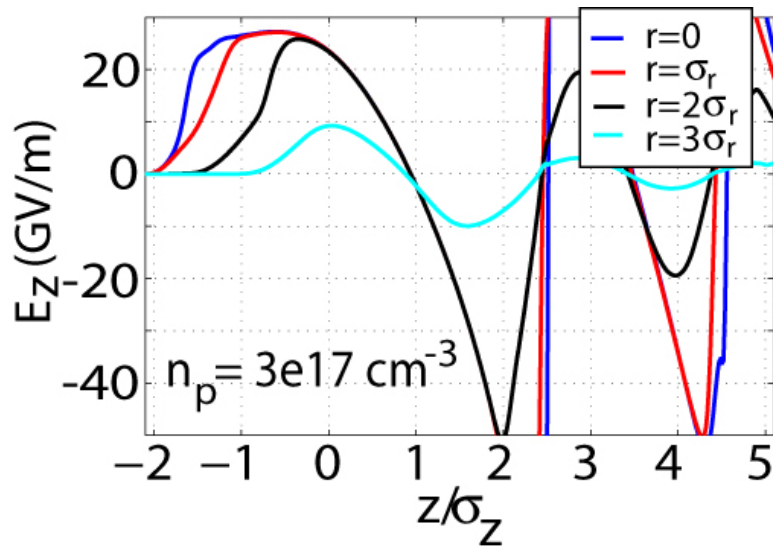
Determined Parameters



- $E_{\text{beam}}=50 \text{ GeV}$, $N_b=4 \times 10^{10}$, $N_p=3 \times 10^{17} \text{ cm}^{-3}$, $\sigma_{x,y}=9 \mu\text{m}$, $\sigma_z=35 \mu\text{m}$, $L_p=1 \text{ m}$

Figure 31: E_z with the parameters listed above.

Table 5: Figure 31 case split into 5 longitudinal bins listing the wakeloss, N_{bi} and the ion column radius for each.



<i>Bin</i>	$N_{bi,x}$	Wakeloss (GeV/m)	$(r_{i,max}/\sigma_r)$
$(-1) - (-.5)\sigma_z$	5.99×10^9	27	2.1
$(-.5) - 0\sigma_z$	7.66×10^9	25	2.6
$0 - .5\sigma_z$	7.66×10^9	18	3.0
$.5 - 1\sigma_z$	5.99×10^9	7	3.0
$1 - 2\sigma_z$	5.40×10^9	-12.5	3.0

Table 6: Results of Simulation: Positrons / incident e^- for plasma IN cases (1-50 MeV)

Case	e^+ collected/ e^-
150 GeV in 35m wiggler (.5 rl W)	~1.5 w/ flux concentrator
50 GeV w/ 1m plasma (.5 rl W)	.44 w/o flux concentrator



Current Experimental Improvements



- The current experiment was run in a regime not optimum for positron production.
- Large wakefields give great acceleration, but reduce the positron yield substantially.
- However, at SABER at SLAC, new experiments could be performed with respectable source results with the existing 30 GeV beam.

Table 6: Calculated parameters for 3 different cases run with $n_{pe}=3 \times 10^{17} \text{ cm}^{-3}$.

Beam Energy (GeV)	30	40	50
Average e^- Energy Loss (MeV)	935.4	2023	3343
Average Photon Energy (MeV)	14.2	22.9	34.9
Photons/Beam e^-	65.8	88.2	95.9
e^+ /Beam e^- (1-30 MeV)	.09	.17	.23
e^+ /Beam e^- (1-50 MeV)	.15	.30	.44



Compilation of Spectrum Parameters



UCLA



- The experimental measurements were used to compile the appropriate parameters for each density.

Table 3: Compilation of pertinent calculation parameters for 3 different densities used in the experiment

Case	1	2	3
Density [cm^{-3}]	1×10^{17}	6.4×10^{16}	3.3×10^{16}
Oven FWHM [cm]	11	14	16
Saddle-Points	6	6	5
Average CTR signal ($1/\sigma_z$)	~ 85	~ 175	~ 300
Ion Column Charge (N_{bi})	7.2×10^9	8×10^9	8.25×10^9
Ion Column ($\sigma_{i,x,y}$ [μm])	4	5	8
Wakeloss (γ_b [GeV/m])	25	15	11